JOURNAL OF THEORETICAL AND APPLIED MECHANICS
41, 2, pp. 323-340, Warsaw 2003

DYNAMIC BEHAVIOUR OF AN AXIALLY MOVING MULTI-LAYERED WEB

Krzysztof Marynowski

Department of Dynamics of Machines, Technical University of Łódź

Zbigniew Kołakowski

Department of Strenght of Materials and Structures, Technical University of Łódź

e-mail: kola@ck-sg.p.lodz.pl

A new approach to the analysis of the dynamic behaviour of an axially moving composite web is presented. The mathematical model of the moving web system constitutes non-linear, coupled equations governing the transverse displacement and stress function. The calculations are carried out for two paperboard structures. The results of numerical investigations show solutions to linearized problems. The effect of paperboard properties and axial transport velocity on flexural and torsional vibrations are presented.

Key words: composite plate, moving web, dynamic stability

Notation

b	–	width of the web
c	–	axial transport speed
E_x	–	Young's modulus along the x-direction
E_y	–	Young's modulus along the y-direction
G	–	shear modulus of the plate material
h	–	thickness of the web
$\mathbf{K}$	–	stiffness matrix for the laminate
l	–	length of the web
N	–	axial stress
S	–	surface of the web
t	–	time

u, v, w – components of the plate displacement in the x, y and z axis direction, respectively
U – kinetic energy
V – internal elastic strain energy
W – work of external forces
x, y, z – Cartesian co-ordinates
$\varepsilon_x, \varepsilon_y, \varepsilon_z$ – strain components
$\kappa_x, \kappa_y, \kappa_z$ – curvature modifications and torsion components
λ – scalar load parameter
ρ – mass density of the web
σ – real part of eigenvalue
ω – natural frequency.

1. Introduction

Axially moving webs in the form of thin, flat rectangular shape materials with small flexural stiffness occur in the industry as band saw blades, power transmission belts, textile tapes or paper and paperboard webs. Excessive vibrations of moving webs increase defects and can lead to failure of the web. In the paper and textile industries involving motion of thin materials, the stress analysis in the moving web is essential for the control of wrinkle, flutter and sheet break. Although the mechanical behaviour of axially moving materials has been studied for many years, little information is available on the dynamic behaviour and stress distribution in an axially moving multi-layered paper and board materials.

Paper and paperboard properties derive from raw materials and paper-making processes. Relatively recent technical developments allow high speed formation of the web in a simultaneous or sequential multi-layered structure like paperboard. Paper is generally considered to be an anisotropic fibrous composite material. Theoretical models describing mechanical properties of paperboard include those based on an thin-walled composite plate structure.

A lot of earlier works in this field focussed on investigations of stationary orthotropic composite plates. A more comprehensive review of the literature can be found in investigations of Chandra and Raju (1973), Dawe and Wang (1994), Jones (1975), Kołakowski and Królak (1995), Loughlan (2001), Matsunaga (2001), Shen and Williams (1993), Walker *et al.* (1996), Wang *et al.* (1987).

On the other hand, one can find in the literature a lot of works on the dynamic investigations of a one-layered axially moving orthotropic web. Re-

cent works in this field analysed non-linear vibrations of an axially moving orthotropic web (Marynowski and Kołakowski, 1999; Marynowski, 1999), equilibrium displacement and stress distribution in non-linear model of an axially moving plate (Lin, 1997), wrinkling phenomenon and stability of the linear model of an axially moving isotropic plate (Lin and Mote, 1996), and stress distribution in an axially moving plate (Wang, 1999).

The aim of this paper is to analyse the dynamic behaviour of an axially moving multi-layered web. Numerical investigations are carried out for a paperboard structure. Paperboard is treated as a thin-walled composite structure in the elastic range, being under axial extension. The differential equations of motion are derived from the Hamilton principle taking into account the Lagrange description, the strain Green tensor for thin-walled plates and the stress tensor. Singular perturbation theory is used to obtain the approximate solution of the governing equations. The numerical method of the transition matrix using Godunov's orthogonalization is used to solve the linearized problems.

2. Formulation of the structural problem

Paperboard is in general composed of several pulp fiber sheets bonded by starch or an adhesive material, and is usually a multi-layered structure. A schematic of a three-layered paper-board macrostructure is shown in Fig. 1, which also depicts the coordinate system. The x-axis refers to the machine direction, the y-axis refers to the cross-section or transverse direction. The machine and cross directions form the plane of the structure, and the z-axis refers to the out-of-plane (or through-thickness) direction. In this paper, the laminate model has been used to describe the mechanical behaviour of paperboard.

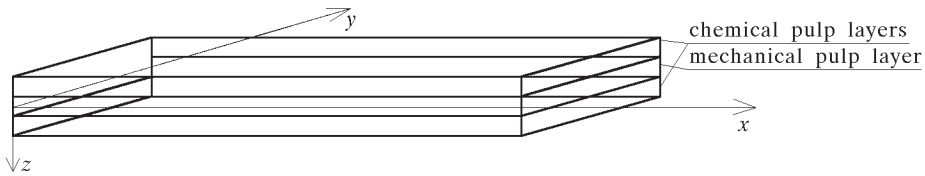

Fig. 1. Schematic of paperboard macrostructure

Let us consider a multi-layer plate element of a thin-walled structure made of orthotropic materials. The classical laminated plate theory (Jones, 1975) is

used in the theoretical analysis, the effects of shear deformation through the thickness of the laminate are neglected and the results given are those for thin laminated plates. The materials they are made of obey Hooke's law.

For each plate component, precise geometrical relationships are assumed in order to enable the consideration of both out-of-plane and in-plane bending of the plate

$$\begin{aligned} &\varepsilon_1 = u_{1,1} + \frac{1}{2}u_{m,1}u_{m,1} && \varepsilon_2 = u_{2,2} + \frac{1}{2}u_{m,2}u_{m,2} \\ &\varepsilon_3 = u_{1,2} + u_{2,1} + u_{m,1}u_{m,2} && \varepsilon_4 = -hu_{3,11} \\ &\varepsilon_5 = -hu_{3,22} && \varepsilon_6 = -2hu_{3,12} \end{aligned} \tag{2.1}$$

where $m = 1, 2, 3$, and $\varepsilon_1 = \varepsilon_x$, $\varepsilon_2 = \varepsilon_y$, $\varepsilon_3 = 2\varepsilon_{xy} = \gamma_{xy}$, $\varepsilon_4 = h\kappa_x$, $\varepsilon_5 = h\kappa_y$, $\varepsilon_6 = h\kappa_{xy}$; $u_1 \equiv u$, $u_2 \equiv v$, $u_3 \equiv w$ are the components of the displacement vector in the $x_1 \equiv x$, $x_2 \equiv y$, $x_3 \equiv z$ axis direction, respectively.

In the majority of publications devoted to stability of structures, the terms $(u_{1,1}^2 + u_{2,1}^2)$, $(u_{1,2}^2 + u_{2,2}^2)$, $(u_{1,1}u_{1,2} + u_{2,1}u_{2,2})$ are neglected for ε_1, ε_2, ε_3, respectively, in the strain tensor components (2.1).

Using the classical plate theory (Jones, 1975), the constitutive equation for the laminate is taken as follows

$$\boldsymbol{N} = \begin{bmatrix} \mathbf{A} & \mathbf{B} \\ \mathbf{B} & \mathbf{D} \end{bmatrix} \boldsymbol{\varepsilon} = \mathbf{K}\boldsymbol{\varepsilon} \tag{2.2}$$

where

$$\begin{aligned} &A_{ij} = \frac{1}{h}\sum_{k=1}^{N}(\overline{Q}_{ij})_k(z_k - z_{k-1}) && B_{ij} = \frac{1}{2h^2}\sum_{k=1}^{N}(\overline{Q}_{ij})_k(z_k^2 - z_{k-1}^2) \\ &D_{ij} = \frac{1}{3h^3}\sum_{k=1}^{N}(\overline{Q}_{ij})_k(z_k^3 - z_{k-1}^3) \end{aligned} \tag{2.3}$$

$$\mathbf{K} = \begin{bmatrix} \mathbf{A} & \mathbf{B} \\ \mathbf{B} & \mathbf{D} \end{bmatrix} = \begin{bmatrix} A_{11} & A_{12} & A_{16} & B_{11} & B_{12} & B_{16} \\ A_{21} & A_{22} & A_{26} & B_{21} & B_{22} & B_{26} \\ A_{61} & A_{62} & A_{66} & B_{61} & B_{62} & B_{66} \\ B_{11} & B_{12} & B_{16} & D_{11} & D_{12} & D_{16} \\ B_{21} & B_{22} & B_{26} & D_{21} & D_{22} & D_{26} \\ B_{61} & B_{62} & B_{66} & D_{61} & D_{62} & D_{66} \end{bmatrix} =$$

$$= \begin{bmatrix} K_{11} & K_{12} & K_{13} & K_{14} & K_{15} & K_{16} \\ K_{21} & K_{22} & K_{23} & K_{24} & K_{25} & K_{26} \\ K_{31} & K_{32} & K_{33} & K_{34} & K_{35} & K_{36} \\ K_{41} & K_{42} & K_{43} & K_{44} & K_{45} & K_{46} \\ K_{51} & K_{52} & K_{53} & K_{54} & K_{55} & K_{56} \\ K_{61} & K_{62} & K_{63} & K_{64} & K_{65} & K_{66} \end{bmatrix}$$

in which $A_{ij} = A_{ji}$, $B_{ij} = B_{ji}$ $D_{ij} = D_{ji}$, $K_{ij} = K_{ji}$, and $\overline{Q}_{ij}$ is the transformed reduced stiffness matrix (Dawe and Wang, 1994; Jones, 1975).

In the above equations the dimensionless sectional forces N_1, N_2, N_3 and the dimensionless sectional moments N_4, N_5, N_6 appear in the following forms

$$\begin{aligned} N_1 &= \frac{N_x}{h} & N_2 &= \frac{N_y}{h} & N_3 &= \frac{N_{xy}}{h} \\ N_4 &= \frac{M_x}{h^2} & N_5 &= \frac{M_y}{h^2} & N_6 &= \frac{M_{xy}}{h^2} \end{aligned} \tag{2.4}$$

In the constitutive matrix of Eq. (2.2), the submatrix **A**, detailed in Eq. $(2.3)_1$ and related to the in-plane response of the laminate, is called the extensional stiffness. The submatrix **D**, described by Eq. $(2.3)_3$, is associated with the out-of-plane bending response of the laminate and is called the bending stiffness, whereas the submatrix **B**, illustrated by Eq. $(2.3)_2$, is a measure of an interaction (coupling) between the membrane and the bending action. Thus, it is impossible to pull on a laminate that has B_{ij} terms without bending and/or twisting the laminate at the same time. This entails that the extensional force results in not only extensional deformations, but also in twisting and/or bending of the laminate (Dawe and Wang, 1994; Jones, 1975). Moreover, such a laminate cannot be subjected to a moment without suffering simultaneously from extension of the middle surface.

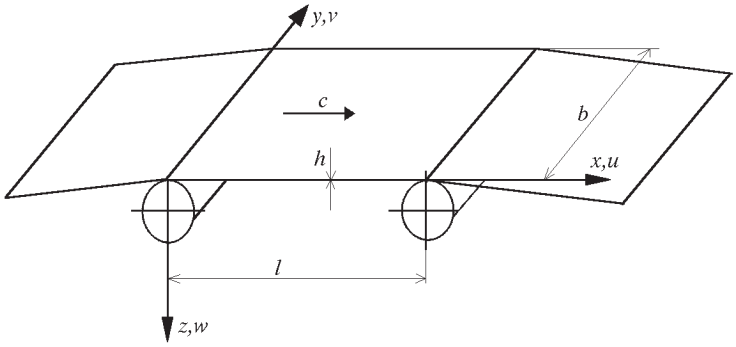

Fig. 2. Axially moving web

Let suppose now that the multi-layered web of the length l is considered. The web moves at the constant velocity c in the x direction. The geometry of the considered model is shown in Fig. 2.

The equations of the dynamic stability of a moving composite structure have been derived using the Hamilton principle, which, for the web, can be written as

$$\delta \int_{t_0}^{t_1} L\, dt = \int_{t_0}^{t_1} (\delta U - \delta V + \delta W)\, dt =$$

$$= \int_{t_0}^{t_1} \Big\{ \frac{1}{2}\rho \int_{\Omega} \delta[(c + u_{1,t} + cu_{1,1})^2 + (u_{2,t} + cu_{2,1})^2 + (u_{3,t} + cu_{3,1})^2]\, d\Omega - \tag{2.5}$$

$$- \frac{1}{2} \int_{\Omega} (\sigma_x \delta\varepsilon_x + \sigma_y \delta\varepsilon_y + \tau_{xy}\delta\gamma_{xy})\, d\Omega + \int_0^b hp^0(x_2)\delta u_1\, dx_2 \Big|_{x_1=0}^{x_1=\ell} \Big\}\, dt = 0$$

where L is the Lagrange function, $\Omega = l \times b \times h = S \times h$, and $p^0(x_2)$ is the pre-critical external load in the plate middle surface.

After grouping the components at respective variations, the following system of equilibrium equations of motion has been obtained

$$\int_{t_0}^{t_1}\int_S \{[N_1(1 + u_{1,1}) + N_3 u_{1,2}]_{,1} + [N_2 u_{1,2} + N_3(1 + u_{1,1})]_{,2} +$$
$$+ \overline{\rho}(-u_{1,tt} - 2cu_{1,1t} - c^2 u_{1,11})\}\delta u_1\, dSdt = 0$$
$$\int_{t_0}^{t_1}\int_S \{[N_1 u_{2,1} + N_3(1 + u_{2,2})]_{,1} + [N_2(1 + u_{2,2}) + N_3 u_{2,1}]_{,2} + \tag{2.6}$$
$$+ \overline{\rho}(-u_{2,tt} - 2cu_{2,1t} - c^2 u_{2,11})\}\delta u_2\, dSdt = 0$$
$$\int_{t_0}^{t_1}\int_S [(hN_{4,1} + N_1 u_{3,1} + N_3 u_{3,2})_{,1} + (hN_{5,2} + 2hN_{6,1} + N_2 u_{3,2} + N_3 u_{3,1})_{,2} +$$
$$+ \overline{\rho}(-u_{3,tt} - 2cu_{3,1t} - c^2 u_{3,11})]\delta u_3\, dSdt = 0$$

where

$$\overline{\rho} = \frac{1}{h}\sum_{k=1}^{N} \rho_k (z_k - z_{k-1})$$

The boundary conditions for $x_1 = \text{const}$

$$\int_{t_0}^{t_1}\int_0^b \Big[\overline{\rho}(c^2 + cu_{1,t} + c^2 u_{1,1}) -$$
$$- (N_1 + N_1 u_{1,1} + N_3 u_{1,2} - hp^0(x_2))\Big]\delta u_1\, dx_2 dt\Big|_{x_1} = 0$$

$$\int_{t_0}^{t_1}\int_{0}^{b}\Big[\overline{\rho}(cu_{2,t}+c^2u_{2,1})-(N_3+N_1u_{2,1}+N_3u_{2,2})\Big]\delta u_2\ dx_2dt\Big|_{x_1}=0$$

$$\int_{t_0}^{t_1}\int_{0}^{b}N_4\delta u_{3,1}\ dx_2dt\Big|_{x_1}=0 \tag{2.7}$$

$$\int_{t_0}^{t_1}\int_{0}^{b}\Big[\overline{\rho}(cu_{3,t}+c^2u_{3,1})-(hN_{4,1}+2hN_{6,2}+N_1u_{3,1}+N_3u_{3,2})\Big]\delta u_3\ dx_2dt\Big|_{x_1}=0$$

The boundary conditions for $x_2 = \text{const}$

$$\int_{t_0}^{t_1}\int_{0}^{l}(N_2+N_2u_{2,2}+N_3u_{2,1})\delta u_2\ dx_1dt\Big|_{x_2}=0$$

$$\int_{t_0}^{t_1}\int_{0}^{l}(N_3+N_2u_{1,2}+N_3u_{1,1})\delta u_1\ dx_1dt\Big|_{x_2}=0 \tag{2.8}$$

$$\int_{t_0}^{t_1}\int_{0}^{l}N_5\delta u_{3,2}\ dx_1dt\Big|_{x_2}=0$$

$$\int_{t_0}^{t_1}\int_{0}^{\ell}(hN_{5,2}+2hN_{6,1}+N_2u_{3,2}+N_3u_{3,1})\delta u_3\ dx_1dt\Big|_{x_2}=0$$

The boundary conditions for the plate corner ($x_1 = \text{const}$ and $x_2 = \text{const}$)

$$\int_{t_0}^{t_1}2N_6\Big|_{x_1}\Big|_{x_2}\delta u_3\ dt=0 \tag{2.9}$$

The initial conditions

$$\int_{0}^{l}\int_{0}^{b}[\overline{\rho}(c+u_{1,t}+cu_{1,1})]\delta u_1\ dx_1dx_2\Big|_{t=0}=0$$

$$\int_{0}^{l}\int_{0}^{b}[\overline{\rho}(u_{2,t}+cu_{2,1})]\delta u_2\ dx_1dx_2\Big|_{t=0}=0 \tag{2.10}$$

$$\int_{0}^{l}\int_{0}^{b}[\overline{\rho}(u_{3,t}+cu_{3,1})]\delta u_3\ dx_1dx_2\Big|_{t=0}=0$$

3. Solution to the problem

The problem of the dynamic stability has been solved by making use of the asymptotic perturbation method. In the solution and in the developed computer program, the following have been employed: Byskov-Hutchinson's asymptotic expansion (Byskov and Hutchinson, 1977), the numerical transition matrix method using Godunov's orthogonalization method (Kołakowski and Królak, 1995).

As has been mentioned above, the fields of displacements $\overline{U}$ and the fields of sectional forces $\overline{N}$ have been expanded into power series with respect to the dimensionless amplitude of the web deflection ζ_n (the amplitude of the nth free vibration frequency of the extension system divided by the thickness h_1 of the web assumed to be the first one)

$$\begin{aligned} \overline{U} &= \lambda \overline{U}_k^{(0)} + \zeta_n \overline{U}_k^{(n)} + ... \\ \overline{N} &= \lambda \overline{N}_k^{(0)} + \zeta_n \overline{N}_k^{(n)} + ... \end{aligned} \tag{3.1}$$

where

$\overline{U}_k^{(0)}, \overline{N}_k^{(0)}$ – pre-critical static fields

$\overline{U}_k^{(n)}, \overline{N}_k^{(n)}$ – first order fields for the composite kth web.

After substitution of expansions (3.1) into equilibrium Eqs. (2.6), continuity conditions and boundary conditions Eqs. (2.7)-(2.9), the boundary value problems of the zero and first order can been obtained.

The zero approximation describes the pre-critical static state, whereas the first order approximation, being the linear problem of the dynamic stability, allows for the determination of the eigenvalues, eigenvectors and the critical speeds of the system.

The panels with linearly varying pre-critical loads along their widths are divided into several strips under uniformly distributed tensile stresses. Instead of the finite strip method, the exact transition matrix method is used in this case (Marynowski and Kołakowski, 1999).

The inertial forces corresponding to the in-plane displacements u and v are neglected. The pre-critical solution of the kth composite web consisting of homogeneous fields is assumed as

$$u_{1k}^{(0)} = -\Big(\frac{\ell}{2} - x_{1k}\Big)\Delta_k \qquad u_{2k}^{(0)} = -x_{2k}\Delta_k \frac{K_{12k}}{K_{22k}} \qquad u_{3k}^{(0)} = 0 \tag{3.2}$$

where Δ_k is the actual loading. This loading is specified as the product of a unit loading and a scalar load factor Δ_k.

The inner sectional forces of the pre-critical static state for the assumed homogeneous field of displacements (3.1) are expressed by the following relationships

$$\begin{aligned}
&\overline{N}_{1k}^{(0)} = -\Big(K_{11} - \frac{K_{12}^2}{K_{22}}\Big)\Delta && \overline{N}_{4k}^{(0)} = -\Big(K_{41} - K_{42}\frac{K_{21}}{K_{22}}\Big)\Delta \\
&\overline{N}_{2k}^{(0)} = 0 && \overline{N}_{5k}^{(0)} = -\Big(K_{51} - K_{52}\frac{K_{21}}{K_{22}}\Big)\Delta \\
&\overline{N}_{3k}^{(0)} = -\Big(K_{31} - K_{32}\frac{K_{21}}{K_{22}}\Big)\Delta && \overline{N}_{6k}^{(0)} = -\Big(K_{61} - K_{62}\frac{K_{21}}{K_{22}}\Big)\Delta
\end{aligned} \tag{3.3}$$

In the one before last dynamical component of Eg. $(2.6)_3$ there is a derivative with respect to x_1 and t. Because of the incompatibility of trigonometric functions in the $x_1 \equiv x$-direction, the Galerkin-Bubnov orthogonalization procedure is used to find an approximating solution to this equation.

Numerical aspects of the problem being solved for the first order fields (Marynowski and Kołakowski, 1999) have resulted in an introduction of the following new orthogonal functions with the nth harmonic for kth composite web in the sense of the boundary conditions for two longitudinal edges

$$\begin{aligned}
&\overline{a}_k^{(n)} = N_{2k}^{(n)}\Big(1 + \lambda\Delta_k\frac{K_{21k}}{K_{22k}}\Big) + \lambda N_{3k}^{(0)}\frac{\overline{d}_{k,\xi}^{(n)}}{b_k} && \overline{d}_k^{(n)} = u_{21k}^{(n)} \\
&\overline{b}_k^{(n)} = N_{3k}^{(n)}(1 - \lambda\Delta_k) + \lambda N_{3k}^{(0)}\frac{\overline{c}_{k,\xi}^{(n)}}{b_k} && \overline{e}_k^{(n)} = u_{3k}^{(n)} \\
&\overline{c}_k^{(n)} = u_{1k}^{(n)} && \overline{f}_k^{(n)} = \frac{u_{3k,\eta}^{(n)}}{b_k} = \frac{\overline{e}_{k,\eta}^{(n)}}{b_k} \\
&\overline{h}_k^{(n)} = h_k\frac{\overline{g}_{k,\eta}^{(n)}}{b_k} + 2h_k\frac{N_{6k,\xi}^{(n)}}{b_k} + \lambda N_{3k}^{(0)}\frac{\overline{e}_{k,\xi}^{(n)}}{b_k} && \overline{g}_k^{(n)} = N_{5k}^{(n)}
\end{aligned} \tag{3.4}$$

where

$$\xi_k = \frac{x_{1k}}{b_k} \qquad \eta_k = \frac{x_{2k}}{b_k}$$

The solutions to Eq. $(2.6)_3$ corresponding to the free support at the segment ends can be written in the following form

$$\begin{aligned}
\overline{a}_k &= \sum_{n=1}^{N} T_n(t)\overline{A}_k^{(n)}(\eta_k)\sin\beta & \overline{b}_k &= \sum_{n=1}^{N} T_n(t)\overline{B}_k^{(n)}(\eta_k)\cos\beta \\
\overline{c}_k &= \sum_{n=1}^{N} T_n(t)\overline{C}_k^{(n)}(\eta_k)\cos\beta & \overline{d}_k &= \sum_{n=1}^{N} T_n(t)\overline{D}_k^{(n)}(\eta_k)\sin\beta \\
\overline{e}_k &= \sum_{n=1}^{N} T_n(t)\overline{E}_k^{(n)}(\eta_k)\sin\beta & \overline{f}_k &= \sum_{n=1}^{N} T_n(t)\overline{F}_k^{(n)}(\eta_k)\sin\beta \\
\overline{g}_k &= \sum_{n=1}^{N} T_n(t)\overline{G}_k^{(n)}(\eta_k)\sin\beta & \overline{h}_k &= \sum_{n=1}^{N} T_n(t)\overline{H}_k^{(n)}(\eta_k)\sin\beta
\end{aligned} \tag{3.5}$$

where

$$\beta = \frac{n\pi b_k \xi}{\ell}$$

and $T_n(t)$ is an unknown function of time, and the eigenfunctions have been determined for the non-moving tensioned web (for $c = 0$).

The eigenfunctions $\overline{A}_k^{(n)}$, $\overline{B}_k^{(n)}$, $\overline{C}_k^{(n)}$, $\overline{D}_k^{(n)}$, $\overline{E}_k^{(n)}$, $\overline{F}_k^{(n)}$, $\overline{G}_k^{(n)}$, $\overline{H}_k^{(n)}$ (with the nth harmonic) are initially unknown functions that will be determined by the numerical method of transition matrices. The obtained system of homogeneous ordinary differential equations has been solved by the transition matrix method, having integrated numerically the equilibrium equations along the circumferential direction in order to obtain the relationships between the state vectors on two longitudinal edges. During the integration of the equations, Godunov's orthogonalization method is employed (Kołakowski and Królak, 1995; Marynowski, 1999). The presented way of solution allows for carrying out a modal dynamic analysis of complex composite webs.

In system of Eq. $(2.6)_3$ for the non-moving, tensioned web, there are two components of the pre-critical loading $\overline{N}_{1k}^{(0)}$ and $\overline{N}_{3k}^{(0)}$. The component $\overline{N}_{3k}^{(0)}$ has an insignificant effect on the value of the critical load in comparison with $\overline{N}_{1k}^{(0)}$.

Let us return to the case of a moving composite web (i.e. for $c \neq 0$). Because of the incompatibility of trigonometric functions in the x_1-direction, after substituting Eq. (3.4) into Eq. $(2.6)_3$ the Galerkin-Bubnov orthogonalization method has been used. In this way, the set of N ordinary differential equations with respect to the function $T_n(t)$ can be determined in the following form

$$\frac{d^2T_m}{dt^2}a_{2m} + \sum_{n=1}^{N}\frac{dT_n}{dt}a_{1nm} + T_m a_{0m} = 0 \qquad m = 1, 2, ..., N \tag{3.6}$$

Substituting new variables into Eq. (3.5) one can receive an autonomous set of $2N$ first order differential equations with respect to time. On the basis

of Eq. (3.6) one can determine eigenvalues, eigenvectors and critical speeds of the moving system.

4. Numerical results and discussion

Numerical investigations were carried out on the basis of the mathematical model, which was presented in the previous sections. First, the calculations results are compared with the available solutions. The comparison of the dimensionless fundamental natural frequencies $(\omega b^2\sqrt{\rho/(Eyh^2)})$ of a simply supported anti-symmetric angle-ply laminate, obtained in the present study and by Jones (1975) is shown in Fig. 3. The following dimensionless numerical data was used: $E_x/E_y = 40$, $G_{xy}/E_y = 0.5$, $\nu_{xy} = 0.25$. The greatest discrepancies in the compared results can be observed for a two-layer laminate. When the number of layers increases there is little and little discrepancy in the compared values.

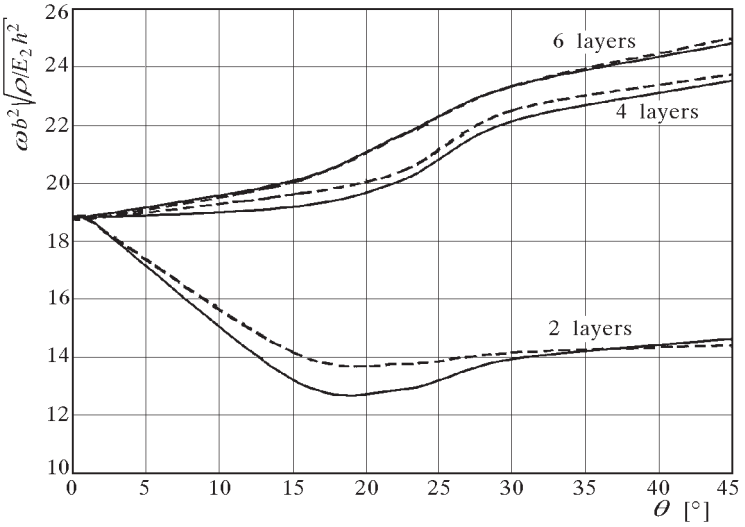

Fig. 3. Comparison of numerical results, θ – play angle, (——) – present study, (– –) – Jones (1975)

The numerical investigations were carried out for a moving paperboard web. The numerical results of the paperboard obtained from the experimental investigations are available in the recent literature (Xia *et al.*, 2002). To recognize the paperboard layers properties, which are not available in approacha-

ble literature, an identification procedure has been employed. Known natural frequencies of a simply supported homogenous paperboard plate model have been compared with analogous values of a three-layered paperboard structure (Fig. 1). Additionally, the outer chemical pulp layers stiffer and stronger than the inner mechanical pulp layer ($E_{1M} = E_{2M} = E_{2C}/100$) was assumed in the identification procedure (Xia *et al.*, 2002). The identification results as the data for the numerical study are shown in Table 1.

Table 1. Numerical data

	System I	System II
Length of the web (l)	1 m	
Width of the web (b)	0.2 m	
Thickness of the chemical pulp layer (h_C)	$3.89 \cdot 10^{-4}$ m	$5.83 \cdot 10^{-4}$ m
Thickness of the mechanical pulp layer (h_M)	$2.22 \cdot 10^{-4}$ m	$3.34 \cdot 10^{-4}$ m
Total thickness of the web	$1 \cdot 10^{-3}$ m	$1.5 \cdot 10^{-3}$ m
Young's modulus along the x-axis of the chemical pulp layer (E_{1C})	5.6 GPa	
Young's modulus along the y-axis of the chemical pulp layer (E_{2C})	2 GPa	
Poisson's ratio in the machine direction of the chemical pulp layer (ν_{12C})	0.392	
Poisson's ratio in the cross direction of the chemical pulp layer (ν_{21C})	0.14	
Shear modulus of the chemical pulp layer (G_C)	34 MPa	
Young's modulus along the machine direction and along the cross direction of the mechanical pulp layer ($E_{1M} = E_{2M}$)	20 MPa	
Poisson's ratio along the machine direction and along the cross direction of the mechanical pulp layer ($\nu_{12M} = \nu_{21M}$)	0.266	
Shear modulus of the mechanical pulp layer (G_M)	7.782 MPa	
Mass density (ρ)	133.33 kg/m^3	
Initial stress ($N_x^{(0)}$)	55 N/m	

The calculations were carried out for two kinds of paperboard web structures of different thickness. The effect of the paperboard properties and axial transport velocity on the transverse and torsional vibrations have been studied in numerical investigations. Let σ and ω denote the real part and imaginary part of the eigenvalues, respectively. Simultaneously, ω is the natural frequency of the web. The positive value of σ indicates instability of the considered system.

At first, eigenvalues of all investigated stationary systems well calculated. Fig. 4 shows the values of the three lowest flexural and flexural-torsional eigenfrequencies of the considered paperboard systems for $c = 0$.

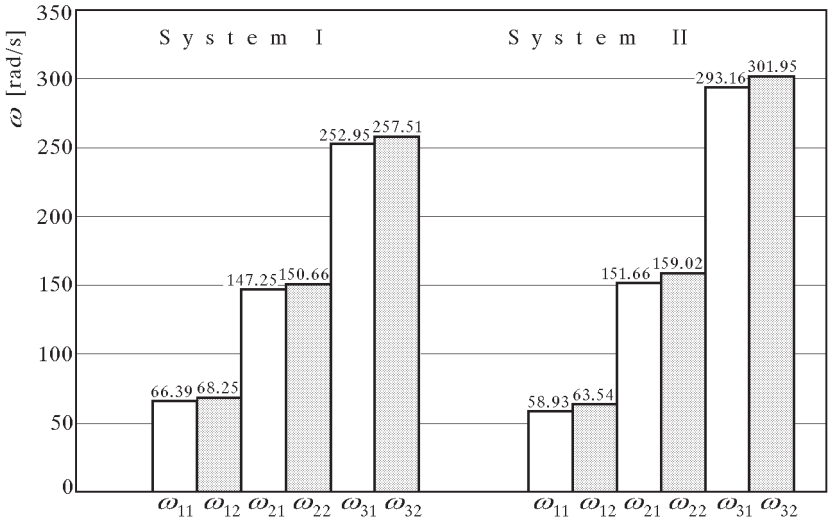

Fig. 4. Three lowest flexural $(\omega_{11}, ..., \omega_{31})$ and flexural-torsional $(\omega_{12}, ..., \omega_{32})$ eigenfrequencies for $c = 0$

The dynamic investigations of the axially moving systems were begun from the vibration modes definition. Fig. 5 shows the modes of the two lowest flexural (ω_{11} and ω_{21}) and two lowest flexural-torsional (ω_{12} and ω_{22}) eigenfrequencies of the considered web systems.

The results of the dynamic stability investigations of web system I for $N = 10$ in Eq. (3.6) are shown in Fig. 6, Fig. 7 and Fig. 8. The values of the imaginary part (solid line) and the real part (dotted line) of the three lowest flexural natural frequencies versus the transport velocity are shown in Fig. 6.

Fig. 7 and Fig. 8 show analogical plots of the flexural and flexural-torsional eigenfrequencies. Both plots in Fig. 5 and Fig. 6 show that in the undercritical region of transport speeds the lowest natural frequencies decrease during the increase in the axial velocity. At the critical transport speed the fundamental eigenfrequency vanishes indicating in divergence instability (the fundamental mode with non-zero σ and zero ω).

For supercritical transport speeds $(c > c_{cr})$, the web experiences at first the divergent instability, and above that there is the second stability area where $\sigma = 0$. In paperboard web system I this region is very narrow (Fig. 8). Its appearance and position is strictly connected with the distribution of the

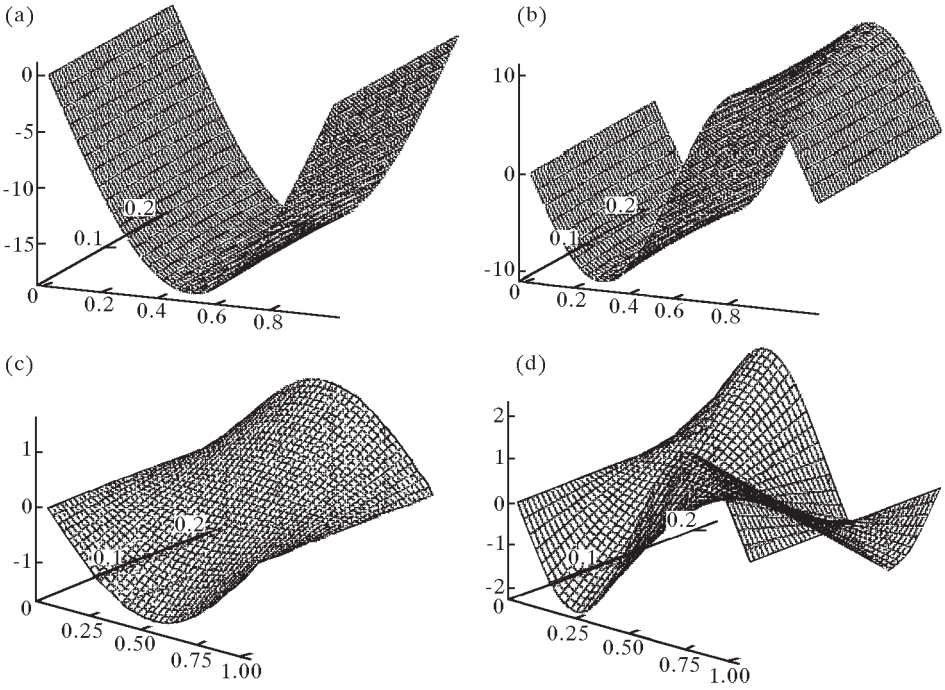

Fig. 5. Non-trivial equilibrium positions of axially moving web: (a) ω_{11}, (b) ω_{21}, (c) ω_{12}, (d) ω_{22}

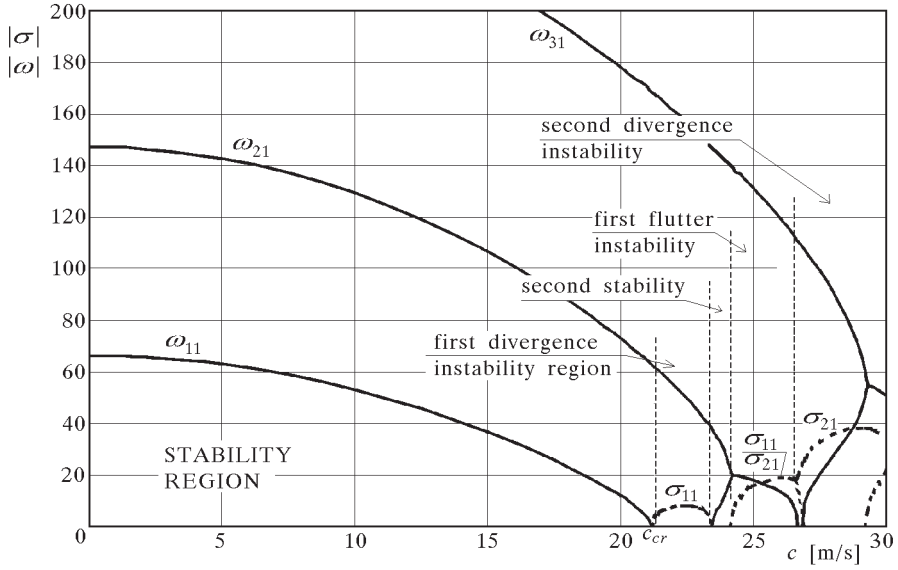

Fig. 6. Flexural natural frequencies (paperboard web system I)

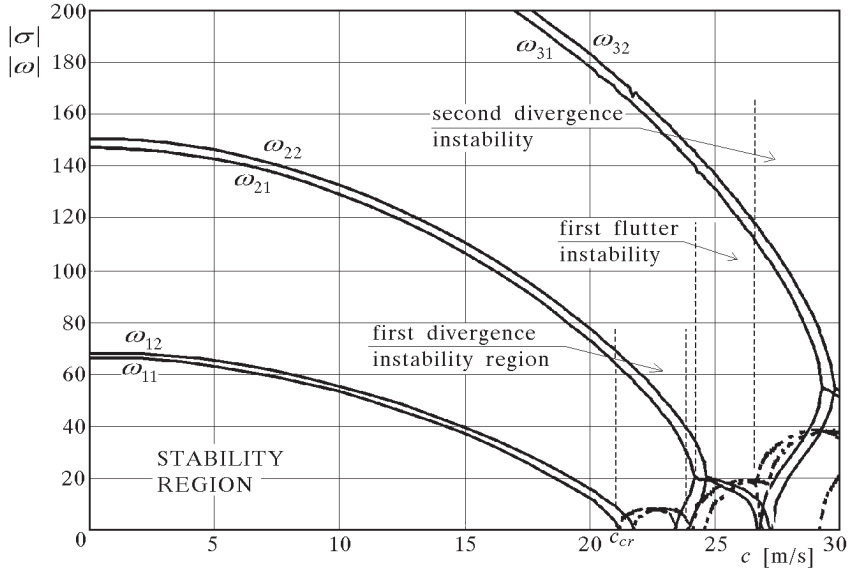

Fig. 7. Flexural and flexural-torsional natural frequencies (paperboard web system I)

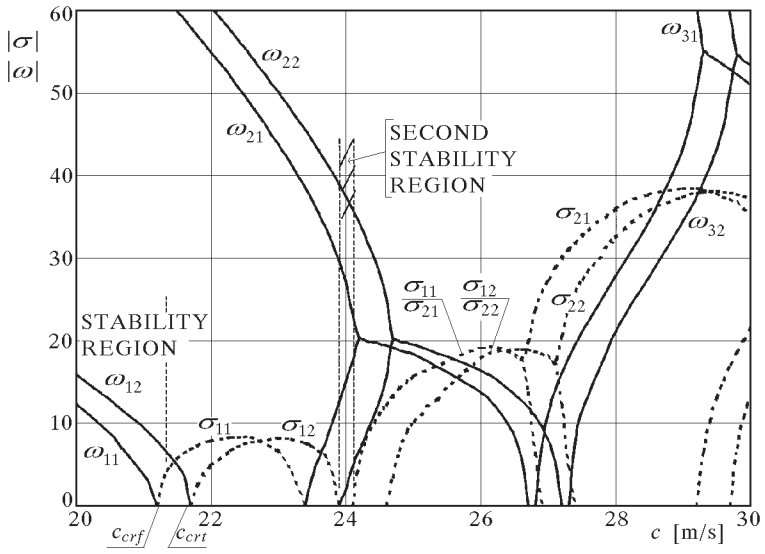

Fig. 8. Flexural and flexural-torsional natural frequencies in the supercritical region (web system I)

flexural and flexural-torsional eigenfrequencies. In the case of paperboard web system II, the second stable area does not appear at all (Fig. 9).

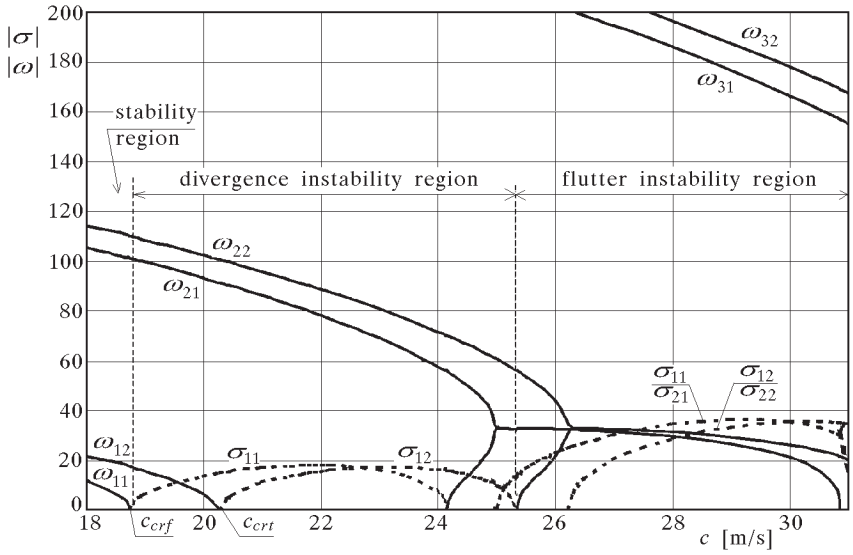

Fig. 9. Flexural and flexural-torsional natural frequencies in the supercritical region (web system II)

Fig. 9 shows a plot of the two lowest flexural and flexural-torsional natural frequencies of web system II in the supercritical region of the transport velocity. The critical transport speed of system II is smaller than in system I. In web system II the distance between the critical transport speed of the flexural vibrations (c_{crf}) and flexural-torsional vibrations (c_{crt}) is greater than in system I, and the second stable area does not appear. Above the divergence instability area there appears a flutter instability region of supercritical transport speeds.

5. Conclusions

In the paper, a new approach to the analysis of the dynamic behaviour of an axially moving multi-layered web is presented. The mathematical model of the moving web system is derived on the basis of the asymptotic perturbation method for the classical laminated thin-walled plate theory. The solution is based on the numerical method of the transition matrix using Godunov's orthogonalization.

The numerical calculations are carried out for two kinds of paperboard web structures. The axially moving paperboard web is treated as a thin-walled composite structure in the elastic range, being under axial extension. The numerical data of the investigated paperboard structure have been received from experimental investigations addressed in literature.

For a constant axial tension of the web, the calculation results show that in the subcritical region of transport speed the lowest flexural and flexural-torsional natural frequencies decrease with growth of the axial velocity. At the critical transport speed the fundamental flexural eigenfrequency vanishes indicating the divergent instability. The critical transport speed of the system is dependent on the thickness of the paperboard layers. The critical speed value decreases when the thickness of the layers increases.

In the supercritical region of transport speed above the divergent instability area the second stable region may appear. The width and position of the second stable region is strictly connected with the distribution of the flexural and flexural-torsional eigenfrequencies. Above the divergent instability and the second stability region there occurs a flutter instability area of supercritical transport speeds.

References

1. BYSKOV E., HUTCHINSON J.W., 1977, Mode interaction in axially stiffened cylindrical shells, *AIAA J.*, **15**, 7, 941-948
2. CHANDRA R., RAJU B.B., 1973, Postbuckling analysis of rectangular ortothropic plates, *Int. Journal of Mechanical Science*, **16**, 81-89
3. DAWE D.J., WANG S., 1994, Buckling of composite plates and plate structures using the spline finite strip method, *Composites Engineering*, **4**, 11, 1099-1117
4. JONES R.M., 1975, *Mechanics of Composite Materials*, International Student Edition, McGraw-Hill Kogakusha, Ltd., Tokyo, 365 p.
5. KOITER W.T., 1976, *General theory of mode interaction in stiffened plate and shell structures*, WTHD, Report 590, Delft
6. KOŁAKOWSKI Z., KRÓLAK M., 1995, Interactive elastic buckling of thin-walled closed orthotropic beam-columns, *Engineering Transactions*, **43**, 4, 571-590
7. LIN C.C., MOTE C.D. JR., 1996, The wrinkling of thin, flat, rectangular webs, *Journal of Applied Mechanics ASME*, **63**, 774-779
8. LIN C.C., 1997, Stability and vibration characteristics of axially moving plates, *Int. Journal of Solid Structures*, **34**, 24, 3179-3190

9. LOUGHLAN J., 2001, The effect of membrane-flexural coupling on the compressive stability of antisymmetric angle-ply laminated plate, *Proceedings of the Third International Conference on Thin-Walled Structures*, Elsevier, 507-514

10. MATSUNAGA H., 2001, Buckling analysis of multilayered angle-ply composite plates, *Proceedings of the Third International Conference on Thin-Walled Structures*, Elsevier, 507-514

11. MARYNOWSKI K., KOŁAKOWSKI Z., 1999, Dynamic behaviour of an axially moving thin orthotropic plate, *Journal of Theoretical and Applied Mechanics*, **37**, 1, 109-128

12. MARYNOWSKI K., 1999, Non-linear vibrations of axially moving orthotropic web, *International Journal of Mechanics and Mechanical Engineering*, **3**, 2, 109-128

13. SHEN H.S., WILLIAMS S.F., 1993, Postbuckling analysis of stiffened laminated panels loaded in compression, *Int. Journal of Solids Structures*, **30**, 12, 1589-1601

14. WALKER M, ADALI S., VERIJENKO V.E., 1996, Optimal design of symmetric angle-ply laminates subject to nonuniform buckling loads and in-plane restraints, *Thin-Walled Structures*, **26**, 1, 45-60

15. WANG C., PIAN T.H.H., DUGUNDJI J., LAGACE P.A., 1987, Analitycal and experimental studies on the buckling of laminated thin-walled structures, *Proc. AIAA/ASME/ASCE/AHS 28th Structures, Struct. Dyn. and Materials Conf.*, Part 1, 135-140

16. WANG X., 1999, Numerical analysis of moving orthotropic thin plates, *Computers and Structures*, **70**, 467-486

17. XIA Q., BOYCE M., PARKS D., 2002, A constitutive model for the anisotropic elastic-plastic deformation of paper and paperboard, *Int. Journal of Solid Structures*, **39**, 4053-4071

Zachowanie dynamiczne poruszającej się osiowo wielowarstwowej wstęgi

Streszczenie

W pracy przedstawiono nową metodę analizy dynamicznej przesuwającej się osiowo kompozytowej wstęgi. Model matematyczny badanego układu wyznaczają nieliniowe, sprzężone równania przemieszczeń poprzecznych oraz funkcji naprężeń. Badania numeryczne przeprowadzono dla dwóch rodzajów wstęgi kartonu. Wyniki tych badań pokazują rozwiązanie problemu liniowego badanego zagadnienia. Przedstawiono wpływ własności kompozytu oraz prędkości przesuwu wstęgi na drgania giętne i giętno-skrętne układu.

Manuscript received October 7, 2002; accepted for print January 17, 2003